Expected CALET Telescope Performance from Monte Carlo Simulations

YOSUI AKAIKE[1], KATSUAKI KASAHARA[1], SHOJI TORII[1], SHUNSUKE OZAWA[1], YUKI SHIMIZU[2], MIKIHIKO KARUBE[1], KEISUKE YOSHIDA[1], KENJI YOSHIDA[3], MASAKATSU ICHIMURA[4]
[1]*Research Institute for Science and Engineering, Waseda University, Tokyo 169-8555, Japan*
[2]*Japan Aerospace Exploration Agency, Tsukuba 305-8505, Japan*
[3]*Department of Electronic Information Systems, Shibaura Institute of Technology, Saitama 330-8570, Japan*
[4]*Faculty of Science and Technology, Hirosaki University, Hirosaki 036-8561, Japan*
Y.Akaike:yosui.a-19@akane.waseda.jp
DOI: 10.7529/ICRC2011/V06/0769

Abstract: The CALorimetric Electron Telescope, CALET, is a versatile detector for exploring the high energy universe, planned to be placed on the Japanese Experiment Module Facility of the International Space Station, ISS. CALET is designed to perform direct measurements of electrons from 1 GeV to 20 TeV, gamma-rays from 10 GeV to 10 TeV, and protons and nuclei from several 10 GeV to 1000 TeV. The main detector consists of a Charge Detector (CHD), an Imaging Calorimeter (IMC), and a Total Absorption Calorimeter (TASC). The total thickness of the calorimeter is 30 X_0 for electromagnetic particles or 1.3 λ for protons. We have been carrying out Monte Carlo simulations with EPICS to study the CALET performance. With its imaging and deep calorimeter, CALET provides excellent proton rejection, $\sim 10^5$, and a high energy resolution, $\sim$2%, over 100 GeV for electromagnetic particles, which make possible the observation of electrons and gamma-rays into the TeV region. In this paper, we will present the expected performance in observing the different particle species, including the geometric factor, the trigger efficiency, the energy resolution and the particle identification power.

Keywords: Cosmic ray electrons, Gamma-rays, Nuclei, Calorimeter, Simulation, ISS

1 Introduction

The CALorimetric Electron Telescope, CALET, is an experiment which will be placed on the Japanese Experiment Module Exposed Facility of the International Space Station (ISS) to measure primary cosmic ray spectra in space for five years [1]. Major scientific objectives are to search for nearby cosmic ray sources and dark matter by carrying out a precise measurement of the electrons from 1 GeV to 20 TeV, the gamma-rays from 10 GeV to 10 TeV, and the protons and nuclei from several tens of GeV to 1000 TeV [2].

In order to optimize and accurately evaluate the CALET performance we have performed Monte Carlo studies using EPICS[1] for observing each of these particle species.

2 The CALET Detector

The CALET detector consists of Charge Detector (CHD), Imaging Calorimeter (IMC), and Total Absorption Calorimeter (TASC). A schematic configuration of the CALET detector is shown in Fig. 1 with an example of a shower profile produced by a 1 TeV electron.

CHD placed on the top of the detector is capable of measuring the charge of incident particles. It is made of two orthogonal layers of plastic scintillator, with each layer segmented into 14 scintillator paddles for the reduction of back scattering effects. Each paddle has a dimension of 32 (W) $\times$ 448 (L) $\times$ 10 (H) mm^3. The detail of CHD is described in an accompanying paper [3].

IMC is composed of 8 layers (*x* and *y* in one layer) of scintillating fiber (SciFi) belts and 7 tungsten plates to detect the particles in the pre-shower stage. The SciFi belt of 448 mm^2 is assembled with 448 SciFis of 1 mm square cross section in each. Each layer consists of two SciFi belts arranged in the *x* and *y* direction. The total thickness of tungsten is three radiation lengths (3 X_0). The five top tungsten plates each have a thickness of 0.1 X_0, and the two lower tungsten each have a thickness of 1.0 X_0. IMC is designed to identify precisely the charge of the incident particle, its first interaction point, and the arrival direction.

TASC, in the current simulation, is composed of 192 PWO scintillators, each of which has a dimension of 20 $\times$ 20 mm^2 in cross section and 320 mm length. They are stacked in 12 layers arranged alternatively in the *x* and *y* direction as a hodoscope. TASC has a thickness of 27.0 X_0 for elec-

1. EPICS stands for Electron-Photon Induced Cascade Simulator in a detector (URL: http://www.cosmos.n.kanagawa-u.ac.jp)

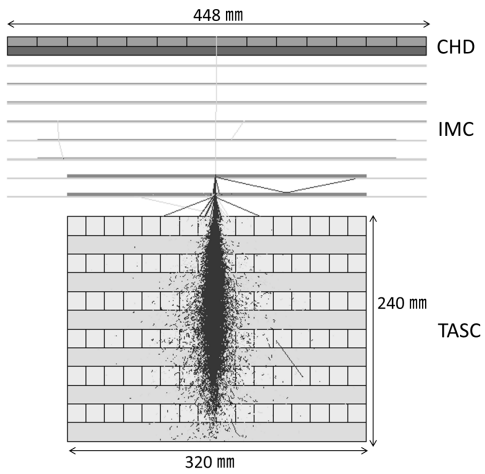

Figure 1: Schematic side view of CALET and an example of simulated shower produced by a 1 TeV electron.

tromagnetic particles or 1.2 λ for protons, and plays a key role for the energy measurement and the electron/proton separation.

CALET is implemented with three trigger sources and can operate in various trigger modes by a combination of these. The first trigger source is the sum of signals from the SciFi belts. The second trigger source is the sum of signals from the top layer in TASC. As the third trigger, we use the sum of signals from the plastic scintillators in CHD.

3 Simulation of the CALET observation

We use EPICS as a Monte Carlo simulation code and adopt dpmjet3 [4] as a hadron interaction model. Isotropic incident particles are assumed with a maximum zenith angle of 60°. For nuclei, the calculation is carried out for four typical species: H, He, N, and Fe.

3.1 Event Trigger

The trigger mode is classified into three categories depending on the target, incident particles, and energy.

- **High energy shower trigger (HES)**
  HES is used to observe all showers over 10 GeV. The threshold for the signal from the top layer in TASC is determined so that 95% of 10 GeV electrons can be detected. As the trigger source in IMC, we use the sum of signals from the 7th and 8th layer SciFi belts, since this trigger observes gamma-rays in addition to charged particles, and detects events entering from the side of the detector. The threshold is set to detect 98% of the 10 GeV gamma-rays for which the first conversion occurs above the 7th layer. This trigger is the primary CALET mission trigger.
- **Low energy shower trigger (LES)**
  LES used for low energy electrons ($>$ 1 GeV) to study solar activity. This trigger will be used at high latitudes where the cutoff rigidity is less than 2 GV. The duration is 5 minutes in every two orbits. All trigger sources are used and each threshold is set to detect 95% of the 1 GeV electrons.
- **Single trigger**
  This trigger detects the minimum ionizing particles (MIPs) for the detector calibration. All trigger sources are used and each threshold is set to detect one MIP signal.

3.2 Event Selection

To evaluate the detector performance, we select events based on the geometry of the shower axis as following. For electrons and gamma-rays, the selection requires that the shower axis passes through both the 4th layer of IMC and the top layer of TASC, and that the axis length in TASC is longer than 24 cm (the thickness of TASC). In addition, for protons and nuclei, the shower axis must pass through CHD, since the CHD information is needed for charge identification. In following analysis, we select only events for which the first interaction occurs above or within the top layer in TASC.

4 Expected Performance

4.1 Trigger Efficiency

Figure 2 shows the trigger efficiency for each kind of particles as a function of energy for the high energy shower trigger. In the high energy region over the threshold, the efficiency for electrons is almost 100% while that for protons is about 20%: The high energy shower trigger selects showering electron events and rejects non-showering proton events very efficiently.

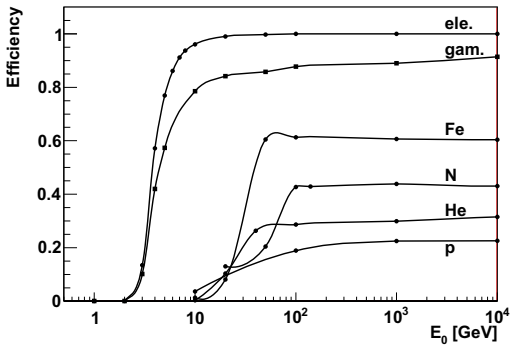

Figure 2: Trigger efficiency of each particles by HES as a function of energy.

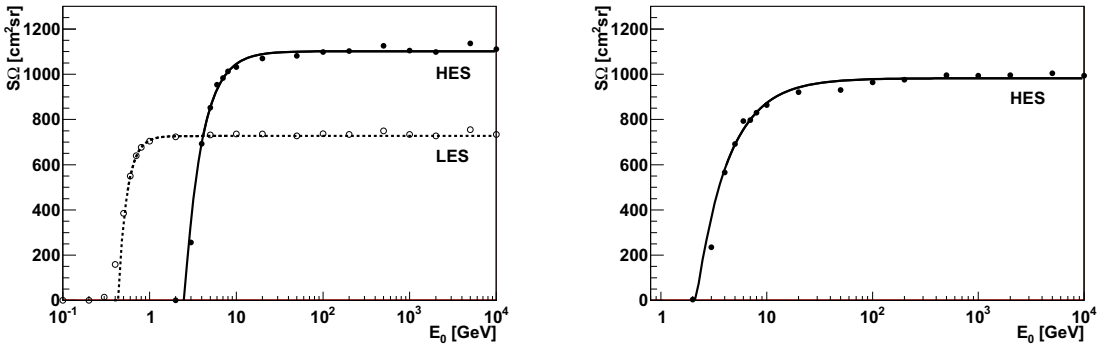

Figure 3: Geometric factor as a function of energy. The left figure is for electrons, and the right is for gamma-rays.

The trigger efficiency for nuclei above several tens of GeV is almost constant. The efficiency for heavier nuclei is higher due to the larger interaction cross-section.

4.2 Geometric Factor

The geometric factor, $S\Omega$, taking account of the trigger efficiency is calculated. Figure 3 shows $S\Omega$ for electrons and gamma-rays as a function of energy. For electrons above 10 GeV observed by HES, $S\Omega \sim 1200$ cm^{2}sr. At energies of 1 GeV - 10 GeV, the electrons are observed by LES, of which the geometry condition of shower axis is limited than that of HES. Therefore, the $S\Omega$ of LES is less than that of HES. Assuming the simple extrapolation of the electron spectrum observed in the Fermi/LAT observation [5], CALET might observe about 1000 electrons over 1 TeV with an exposure of 220 m^2 sr day.

The $S\Omega$ of gamma-rays is nearly 1000 cm^{2}sr, which is less than that of electrons because the pair creation of gamma-rays has to occur above the 7th SciFi layer to carry out the precise determination of the incident direction.

4.3 Energy Resolution

The incident energy is determined by the sum of the energy deposited in IMC and TASC. The energy resolution for electrons and gamma-rays is presented in Fig. 4(left). We note that the energy resolution above 100 GeV is excellent, $\sim 2\%$, due to a very thick absorber. This resolution will enable us to detect any distinctive feature in the energy spectrum originating from dark matter or astrophysical origins at sub-TeV energies.

Figure 4(right) shows the energy resolution for protons and nuclei as a function of incident energy. We can expect that the resolution becomes better for heavier projectiles because the shower development for heavier particles is expected to fluctuate less. This tendency is seen as we move from protons to He and N. However, for heavy particles like Fe, this does not hold: When the target contains light elements such as H (hydrogen) in SciFi and heavy elements like W, the number of secondary π^0 is different for collisions with H or W targets. This difference leads to dispersive energy deposit in the calorimeter. The resolution for protons is $\sim 30\%$ and for other particles somewhat less than 30% without the dependence on the energy.

4.4 Electron / Proton Separation

Protons are the largest source of background for the high energy electron observation. As the ratio of protons to electrons increases at higher energies, excellent proton rejection power is required. For example, at 10 GeV and 1 TeV energy, the proton intensity is higher than the electron intensity by a factor of 100 and 1000, respectively. Therefore, to suppress the proton contamination below a few percent at TeV region, proton rejection is necessary to be 10^5 for the low background observation of electrons.

To estimate the proton rejection power at 1 TeV, we have simulated 1.6×10^6 proton events with power index -2.7 and energies from 1 TeV to 100 TeV. These protons generate the background events only if they produce energy deposit falling in the same region as 1 TeV electrons.

We distinguish electrons and protons from the different shower development in TASC. The lateral distribution of the electromagnetic cascade shower is generally narrower than that of hadronic cascade shower due to the spread of the secondary hadrons. On the contrary, the electromagnetic cascade shower develops earlier than the hadronic cascade shower. CALET has a thick absorber for electrons and a relatively thin absorber for protons. Therefore, at the bottom layer of TASC, electron showers die out, whereas hadronic showers are usually still developing. To distinguish electrons from protons, we used the energy weighted spread as a measure of the lateral spread and the fraction of energy deposited at the bottom layer as a measure of the longitudinal profile:

$$R_E = \sqrt{\frac{\sum_i (\sum_j \Delta E_{i,j} \times R_i^2)}{\sum_i \sum_j \Delta E_{i,j}}} \quad (1)$$

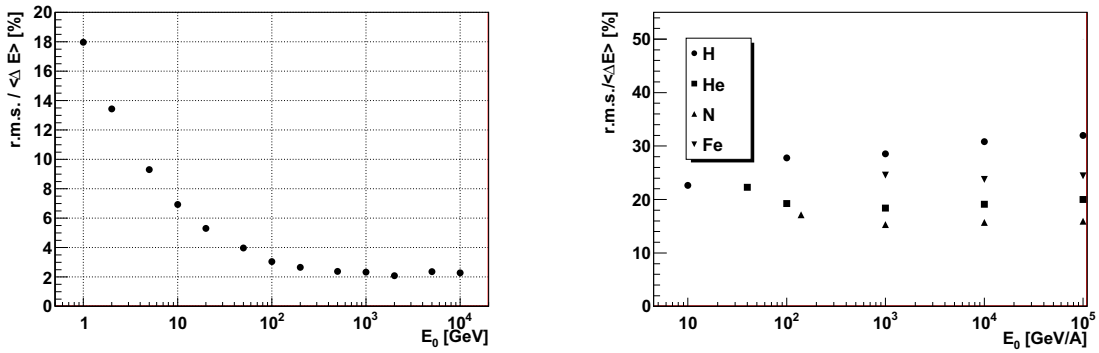

Figure 4: Energy Resolution as a function of energy. The left figure is for electrons. The resolution of gamma-rays above 10 GeV is very similar to that of electrons. The right figure is for protons and nuclei.

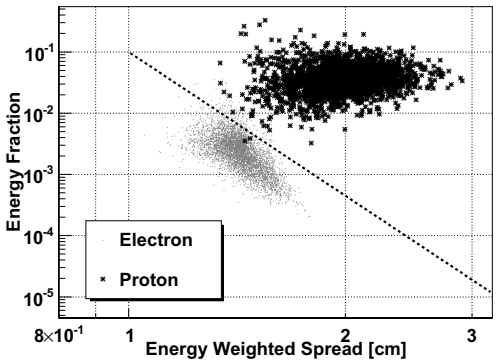

Figure 5: The scatter plots of R_E vs. F_E for electrons and protons. The dots under the line are electrons and the cross points are protons. The events in the left-down region below dashed line can be selected as electrons.

$$F_E = \frac{\sum_j \Delta E_{12,j}}{\sum_i \sum_j \Delta E_{i,j}} \tag{2}$$

where $\Delta E_{i,j}$ is the energy deposited in the ith layer and the jth PWO crystal. R_i is the r.m.s. spread at the ith layer,

$$R_i = \sqrt{\frac{\sum_j (\Delta E_{i,j} \times (x_{i,j} - x_{i,c})^2)}{\sum_j \Delta E_{i,j}}} \tag{3}$$

where $x_{i,c}$ is the coordinate of the shower axis in the ith layer reconstructed in IMC, and x_j is the coordinate of the center of the ith layer and jth PWO crystal.

Figure 5 shows the scatter plots of R_E vs. F_E for electrons with energy of 1 TeV vs. protons in 1 - 100 TeV. Since the distribution of events in the scatter plot depends on the geometry of the shower axis, we classify events into four cases by the geometry in order to distinguish electrons from protons more effectively. In total, the cuts retain 95% of the electron events and four proton events in the electron region. As a result, assuming Poisson distribution, the lower limit of the proton rejection power in TeV energy region is 2.0×10^5 (90% C.L.).

Table 1: Performance of electrons

$S\Omega$ [cm^{2}sr]	1200
Energy resolution [%]	$\sim$2 ($>$100 GeV)
Proton rejection power	2.0×10^5

5 Summary

We have evaluated the performance of CALET with Monte Carlo simulations. CALET has the capability to observe electrons with high statistical precision, excellent energy resolution, and a high proton-rejection power, as shown in Table 1. We are presently working to evaluate the CALET performance in more details with a full flight structure model.

Acknowledgments

We acknowledge support for a part of this present calculation to the Institute of Cosmic Ray Research, University of Tokyo. This work was supported by a Grant-in-Aid for JSPS Fellows.

References

[1] S. Torii *et al.* , OG1.5 in this proceedings.
[2] K. Yoshida *et al.* , OG1.5 in this proceedings.
[3] Y. Shimizu *et al.* , OG1.5 in this proceedings.
[4] S. Roesler, R. Engel, J. Ranft, Report SLAC-PUB-8730, http://sroesler.web.cern.ch/sroesler/dpmjet3.html
[5] A. A. Abdo *et al.* , Phys. Rev. Lett., 2009, **102**, 181101